UPGRADE LIMITATIONS FOR LHC LAMBERTSON SEPTA FOR FCC

A. Sanz Ull*[1], M. Atanasov, B. Balhan, J. Borburgh. CERN, Geneva, Switzerland
[1]also at Eindhoven University of Technology, Eindhoven, Netherlands

Abstract

The FCC imposes challenging requirements for the injection and extraction septa magnets, given the high beam rigidity, small aperture and constraints from the lattice. The baseline design uses Lambertson septa in a two plane scheme based on the LHC injection and extraction septa. The limitations of Lambertson septa are investigated in terms of maximum field and septum thickness whilst maintaining a low leak field. Energy consumption is explored and a super ferric variant is considered in this context. An optimised design of Lambertson septa is proposed for the FCC injection.

BRIEF DESCRIPTION OF LHC MSD MAGNETS

In each LHC dump line there are 15 Lambertson septa modules, each 4.46 m long, electrically connected in series. There are 5 modules of the MSDA magnets, followed by 5 MSDB and 5 MSDC downstream. The differences between the three families are the septum blade thickness and the number of turns of the coil. The relevant characteristics of the main MSD septum magnets are summarized in Table 1. The leak field values have been estimated from the magnetic flux calculated using FLUX 2D [1].

Table 1: Main characteristics of the LHC MSD septa magnets.

Parameter	**MSDA**	**MSDB**	**MSDC**
Number of magnets	5	5	5
Length (m)	4.46	4.46	4.46
Septum blade thickness (mm)	6	12	18
Current (A)	880	880	800
Number of turns	32	40	48
Field in the gap (T)	0.79	0.99	1.16
Leak field (T)	$< 10^{-6}$	$< 10^{-6}$	$< 10^{-6}$

LAMBERTSON SEPTA FOR THE FCC

The baseline FCC injection layout is an LHC-like injection scheme, with three Lambertson septa families with different septum thickness and magnetic field. The different magnetic field is created by the different number of turns of the coil. It has been shown in [2] that the limitation of Lambertson septa is the saturation of the septum blade. As the iron in the septum blade region starts to saturate, the leak field will increase as a result of the decrease in the iron permeability. The upper half of the magnetic circuit of a Lambertson septum is shown in Fig. 1.

* alejandro.sanz.ull@cern.ch

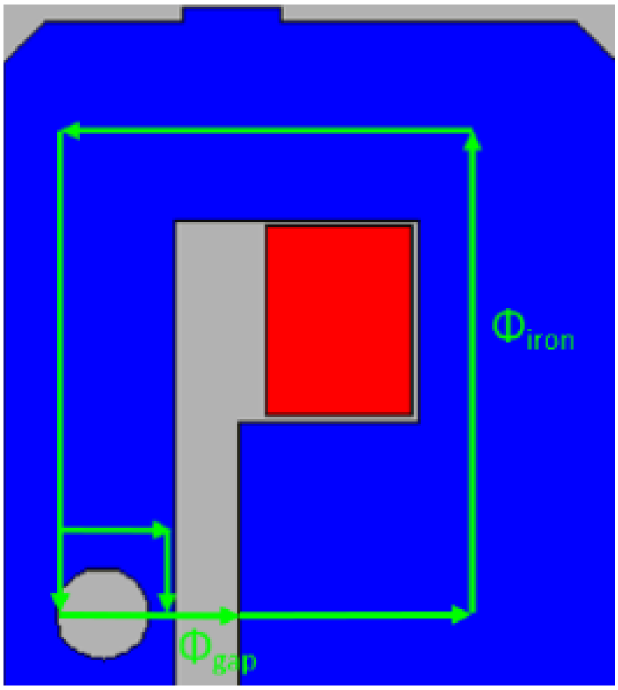

Figure 1: Magnetic circuit of Lambertson septum

The relevant characteristics of the main FCC MSD septum magnets are summarized in Table 2 [3].

Table 2: Main characteristics of the baseline FCC MSD septa magnets.

Parameter	**FCC-A**	**FCC-B**	**FCC-C**
Number of magnets	7	6	5
Length (m)	4.46	4.46	4.46
Septum blade thickness (mm)	8	12	18
Current (A)	1043	1043	1043
Number of turns	288	288	288
Field in the gap (T)	0.7	1	1.2
Leak field (mT·m)	1.4	2.1	2.3

The maximum leak field is calculated from Eq. (1) [4], where $\triangle y$ is the transverse alignment error and α and β are the Twiss parameters. The goal is to calculate $\triangle y' = \frac{\int Bdl}{B\rho}$ in order to obtain a maximum affordable value for the integral leak field. The transverse alignment error is taken as 0.2 mm, which is 33% higher the allowed transverse alignment error in the LHC [5]. The beam emittance and the beam parameters are available in [6] and the Twiss parameters have been calculated using MAD-X. At the extraction point, the parameters of the X-axis and the Y-axis are similar and only an average at the middle point of the allocated length for the septa has been calculated. The values introduced in Eq. (1) are summarized in Table 3. It is assumed that an increase of the beam emittance of 1% is allowed due to the leak field. This is a reasonable value but it is chosen arbitrary, which is acceptable at an early stage of the project. However, the choice has to be made carefully. If the value chosen is too high, there is a risk that the leak field will be too big and ultimately the performance of the accelerator will be degraded. If the value is too low the problem is over-constrained, which is not desirable either. As a further simplification, the alignment term of the equation could be neglected because it is one order of magnitude smaller than the leak field term. However, neglecting this term adds to the uncertainty of the solution calculated this way, therefore the term has been taken into account.

$$\varepsilon_2 = \varepsilon_1 + \frac{\pi}{2} \cdot \left((\triangle y)^2 \, \frac{(1+\alpha^2)}{\beta} + (\triangle y')^2 \beta \right) \qquad (1)$$

Table 3: Parameters used for the emmittance growth calculation.

Parameter	Value
Normalized initial beam emittance (μm)	2.2
Allowed emittance increase due to leak field (%)	1
Alignment error ($\triangle y$) (mm)	0.2
α_x (-)	-1.7
β_x (m)	1594
α_y (-)	1.8
β_y (m)	1740
Beam rigidity at extraction (B·ρ) (T·km)	166.8
Beam rigidity at injection (B·ρ) (T·km)	11

Solving Eq. (1) with the values for the X- axis, one obtains: $\triangle y' = \frac{\int Bdl}{B\rho} = 1.63 \cdot 10^{-6}$. With the beam rigidity at extraction, the leak field integral obtained is $272\, mT \cdot m$. If one takes the value of the beam rigidity at injection, the leak field integral obtained is much smaller ($30\, mT \cdot m$) but this is not a relevant value since the main field in the septum will be much smaller and the leak field in each magnet will be negligible, which ensures that the leak field is below the limit calculated with Eq. (1).

Solving Eq. (1) with the values for the Y-axis produces a maximum leak field integral of $260\, mT \cdot m$, which is a very similar value. Since this calculation starts from the approximation of considering only one septum magnet instead of the real system, only the value for the X-axis will be used.

The leak field value per magnet has been calculated for clarification purposes only. The beam is perturbed by the integral of the magnetic field ($T \cdot m$) while most people find it easier to think in terms of magnetic flux density (T). The value taken as a leak field limit will be the integral field.

Once the maximum leak field that is allowed is known and the septum thickness for each family is fixed, the magnetic field achieved by every magnet family can be calculated. The septum thickness of each family will be determined by the extracted beam separation achieved at every point in the straight section. Allowing to place septa with a thinner septum blade close to the upstream kicker and quadrupole magnet and therefore accumulating the deflection produced by the magnetic field over a longer lever arm. A method to optimize the location of the different septa families and a way to calculate the optimum number of families to be used are shown in [2]. From experience, magnet designers are aware that it is not advisable to manufacture an excessive amount of different magnet families, as the unit cost would increase, because different tooling needs to be produced for every magnet family. However, using too few magnet families may result in having to produce more magnets than necessary in total, increasing the space and power required. The optimum number of magnet families for a given extraction line is found to be two or three. The method developed only considers the magnetic strength and location of each family and therefore for each case the two alternatives must be considered, with any specific constraints that may be present in each particular case. However, this method narrows the possibilities to only two or three families, limiting the number of iterations to study by magnet designers and beam physicists.

The beam size is considered to have a radius from the centre of 15 σ and an additional external tolerance for orbit and alignment is taken as 4 mm, as indicated in Eq. 2. The dimension of σ is given by Eq. 2, where $\beta_{x,y}$ is the beta function in the x and y axis respectively and β_{rel} is the relativistic beta parameter, which at FCC energies can be considered to be one. $D_{x,y}$ is the dispersion and $\Delta p_{x,y}/p_{x,y}$ is the momentum spread. This term can be neglected because its contribution to the beam size is not significant compared to the square root term. The momentum spread, as quoted in the FCC conceptual design report (CDR), is $1.1 \cdot 10^{-4}$ [7], and the maximum dispersion is in the order of 3.3 m. Therefore, the maximum contribution of this term to the beam size is in the order of a fraction of a mm (0.36 mm). The square root term is in the order of a few mm, depending on the location, which means that the dispersion term does not contribute significantly to the size of the beam envelope.

The parameter γ_{rel} is the relativistic gamma parameter, which is 3318 at injection energy and 50272 at extraction. This parameter was calculated using the energies reported in [3] and the rest mass of the proton. The normalized emittance is 2.2 $\mu m \cdot rad$. The beam size is calculated for both the x and y axes according to Eq. (2), which has been reproduced here due to its relevance [8]. This is illustrated in Fig. (2).

$$\begin{gathered} r = 15\sigma + 4\ mm \\ \sigma_{x,y} = \sqrt{\frac{\beta_{x,y}\epsilon_{nx,y}}{\beta_{rel}\gamma_{rel}} + \left(D_{x,y}\frac{\Delta p_{x,y}}{p_{x,y}}\right)^2} \end{gathered} \qquad (2)$$

INJECTION LAYOUT USING TWO AND THREE SEPTA FAMILIES

In order to optimize the septa section it is possible to set up a full optimization problem with the goal function of reducing the total length, including septa magnetic length and drift

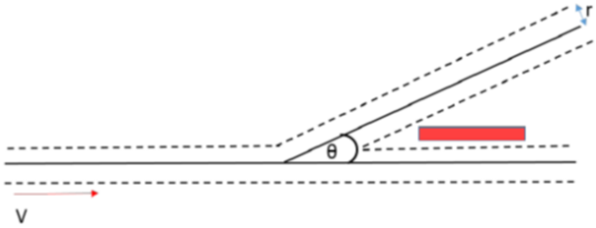

Figure 2: Schematic of the beam size

space length. However, given that the number of magnets is an integer and the necessary deflection constraint is an equality constraint, the solution becomes significantly harder than in the case of linear optimization. Solving the linear case and approximating the integer solution iteratively is an option, although time consuming. Besides, the constraints involving inter-magnet length or minimum drift spaces length have to be introduced with a value that may be arbitrary. The best approach, given that only the two and three families variants are considered is to optimize the septa straight section sequentially. First, the magnetic field and septum blade thickness of each family is decided. This determines the minimum position at which the first magnet of each family can be located. Then the strategy consists of optimizing the total length of each magnet family and the drift space immediately downstream. The process is repeated until the last stage is optimized. Since no constraints are introduced because the optimization is done manually, the result may produce negative value lengths of a given drift space. This can be interpreted as an overdeflection that needs to be compensated. In this case, it is necessary to choose a feasible value for both lengths, as close as possible to the optimum found. The deflection produced by a magnet family is given by Eq. (3), where B is the magnetic field, l_s is the total septa magnetic length and $B\rho$ is the beam rigidity. θ is the deflection angle [9].

$$B \cdot l_s = \theta \cdot B\rho \tag{3}$$

This optimization process has been performed for the two and three families case and the results are compared with the baseline option in Table 4. Like in the LHC, the ratio between magnetic and physical length in the LHC is taken as 0.9 [10]. L_A, L_B and L_C are the lengths of the A, B and C septa families. L_{AB} and L_{BC} are the length of the drift spaces in between the corresponding septa families. L_{QA} is the drift space length between the quadrupole and the first Lambertson septum of family A. L_2 is the drift space immediately following family B or C. It was found that the best option is to allow for a 0 m drift space between each magnet family. Given that this is not possible, a length of 1 m has been chosen to allow for vacuum chamber equipment and supports. Additional constraints, if they may exist, should be taken into account although the principle of the optimization process remains the same. To avoid unfair comparisons, the same 1 m length has been used for every option.

Table 4: Physical lengths of the injection septa system with three Lambertson septa families.

Parameter	2 families	3 families	Baseline
L_{dQA} (m)	27.3	27.3	51.5
L_A (physical)	30.7	30.7	8
L_{AB} (m)	1	1	1
L_B (physical)	55.5	24.2	24
L_{BC} (m)	-	1	1
L_C (physical)	-	22.2	52
L_2 (m)	47.8	61.7	38.7
Total length (m)	161.3	168.1	176.2

Considering a magnetic length of 4 m, as in the case of the LHC, the necessary number of magnets for each option is compared in Table 5.

Table 5: Physical lengths of the injection septa system with three Lambertson septa families.

Parameter	2 families	3 families	Baseline
Number of magnets A	7	7	2
Number of magnets B	13	6	6
Number of magnets C	-	4	13
Total number of magnets	20	18	21

CONCLUSIONS

It can be seen that from the point of view of the number of magnets, it is interesting to use 3 different families of Lambertson septa with the dimensions presented in this study, as the proposal in the baseline requires 3 units more and only uses 2 magnets of the first family, increasing the unit cost of the production.

Although it is not shown in Fig. 2, there needs to be a passive protection device upstream from the injection quadrupole magnet. This device is different than the protection device that protects the extraction septa as it needs to protect the quadrupole magnet and not the septum blade. Space is reserved in the lattice for this device [11] and therefore it is not considered in this study.

Although it has not been shown in this article, the integrated leak field of every option is well below the allowed limits calculated using Eq. (1). A full study of the injection septa optimization and the leak field of every option can be found in [2].

REFERENCES

[1] M. Gyr. in *LHC Project note 129*, Expected Magnetic Field Quality of the LHC Septum Magnets used for Injection (MSI) and for Extraction to the Beam Dump (MSD)

[2] A. Sanz Ull in *Optimization of the magnetic septa for FCC-hh*. PhD thesis, TU Eindhoven, 2019.

[3] M. Benedikt et al. in *FCC Conceptual Design Report*. To be published.

[4] CAS Third general accelerator physics course. Various Authors. 1988.

[5] D. Missiaen in *Alignment and metrology- requirements and realisation*. Proceedings of the CAS: Beam dynamics and technologies for future colliders. Zurich, 2018. https://cas.web.cern.ch/sites/cas.web.cern.ch/files/lectures/zurich-2018/surveyalignment.pdf

[6] F. Zimmermann et al. in *Beam dynamics issues in the FCC*. CERN report 2016-0101. http://cds.cern.ch/record/2200293

[7] X. Buffat, D. Schulte in *Beam parameters evolution and luminosity performance*. FCC Week 2016, Berlin. https://indico.cern.ch/event/438866/contributions/1085031/attachments/1255836/1853844/BeamParameterEvolution-expanded.pdf

[8] E. Wilson in *An Introduction to Particle Accelerators*. Oxford University Press. ISBN 9780198508298. https://books.google.fr/books?id=h0seyyFa394C

[9] D. Tommasini. *Practical definitions and formulae for normal conducting magnets* in TE department internal note. EDMS number 1162401

[10] O. Bruning et al. in *LHC Design Report*, CERN Yellow Reports, 2004. https://cds.cern.ch/record/782076

[11] A. Lechner in *FCC-hh protection absorbers and dumps*. FCC Week 2018, Amsterdam. https://indico.cern.ch/event/656491/contributions/2930779/attachments/1629787/2597491/2018_10_04_fccabsorbersdump.pdf